Combustion and Flame 000 (2018) 1–8

Contents lists available at ScienceDirect

Combustion and Flame

journal homepage: www.elsevier.com/locate/combustflame

Tuning the morphological, ignition and combustion properties of micron-Al/CuO thermites through different synthesis approaches

Sili Deng[a,b,1], Yue Jiang[c,1], Sidi Huang[a], Xinjian Shi[a], Jiheng Zhao[a], Xiaolin Zheng[a,*]

[a] Department of Mechanical Engineering, Stanford University, Stanford, CA 94305, USA
[b] Department of Mechanical Engineering, Massachusetts Institute of Technology, Cambridge, MA 02139, USA
[c] Department of Materials Science and Engineering, Stanford University, Stanford, CA 94305, USA

ARTICLE INFO

Article history:
Received 9 October 2017
Revised 8 March 2018
Accepted 21 April 2018
Available online xxx

Keywords:
Energetic materials
Thermites
Synthesis
Ignition
Combustion

ABSTRACT

Aluminum (Al)-based thermite, due to its high energy density and low cost, has found wide applications in aerospace propulsion, explosion, pyrotechnics, thermal batteries, and power generations. Though significant efforts have been devoted to improving the ignition and combustion performance of Al-based thermites by using nano-Al, micron-Al (m-Al) remains of practical importance over nano-Al due to its lower cost and smaller dead mass. For m-Al based thermite, the main approach to improve its ignition and combustion performance is to bring Al and metal oxide as close as possible to facilitate the oxidizer diffusion process. Herein, we demonstrated two simple synthesis methods, *i.e.*, the precipitation (PC) method and displacement (DP) method, to prepare m-Al/CuO thermites with the intention to bring Al and CuO to shorter diffusion distance and achieve better dispersion. The PC-thermites have flocculent nanostructured CuO closely attached to the surface of m-Al, and the DP-thermites have a dense shell of CuO coated on the surface of m-Al. Both PC- and DP-thermites have reduced agglomeration and diffusion distance over the traditional mechanically mixed (MM)-thermites that have randomly distributed and agglomerated CuO and m-Al. Consequently, both PC- and DP-thermites exhibit shorter ignition delay time, lower reaction onset temperatures, higher heat release, larger pressure rise, and extended reactivity limits than MM-thermites. Particularly, PC-thermites, due to their flocculent structures, exhibit the shortest ignition delay time, lowest reaction onset temperature, and highest amount of heat release. Moreover, the superior ignition and combustion performance of PC- and DP-thermites is more pronounced under high heating rates over low heating rates. Similar PC and DP methods are applicable to prepare diverse thermites with reduced diffusion distance and improved dispersion to improve their ignition and combustion properties.

1. Introduction

Energetic materials composed of metal and metal oxide mixtures (*e.g.*, Al and CuO) are generally referred as thermites. Thermites have high energy density and large post-combustion temperature and pressure rise, so they are extensively utilized to provide heat and thrust in explosion, pyrotechnics, thermal batteries, and power generation [1–4]. Nevertheless, thermites are difficult to ignite and have slow energy release rates and incomplete reaction, hindering them from reaching their full potential in those applications. Those drawbacks of thermites come from two main reasons. Thermite reaction is a heterogeneous reaction that requires the diffusion of oxidizer in the condensed phase, which is inherently slow [5–7]. Furthermore, as the metal fuel is oxidized, the generated metal oxide accumulates on the surface of metal, inhibiting the further diffusion of the oxidizer into the metal [8,9].

To facilitate the diffusion process, a general approach is to reduce the diffusion distance by bringing metal fuel and metal oxide as close as possible and/or reducing the size of components to nanoscales [10]. Following these principles, much research effort has been devoted to the synthesis and characterization of nano-sized thermites (nanothermites). A recent review by Dreizin [11] summarized different synthesis methods for preparing nanothermites, including powder mixing [12–15], sol–gel [15,16], self-assembly [17–20], layered vapor deposition [21–24], and arrested reactive milling (ARM) [25,26]. In brief, the powder mixing method is also known as the mechanical mixing (MM) method, in which the component particles are physically mixed with or without liquid carrier. In the sol–gel processing, the fuel particles are imbedded in the pores of the oxidizer matrix to form a nanocomposite. For the self-assembly, surfactants are utilized to functionalize the

---

[*] Corresponding author.
E-mail address: xlzheng@stanford.edu (X. Zheng).
[1] Sili Deng and Yue Jiang contributed equally to this work.

https://doi.org/10.1016/j.combustflame.2018.04.028
0010-2180/© 2018 The Combustion Institute. Published by Elsevier Inc. All rights reserved.

surface of component particles to achieve ordered arrangements. In the layered vapor deposition, component layers are coated on top of each other using vacuum deposition, forming layered nanofoils. In arrested reactive milling, the feedstocks are often micron-sized components and are refined to nanocomposites in a ball-milling reactor.

In spite of the high reactivity of nanothermites, the production of nano-Al (n-Al) is rather energy-intensive and costly [27]. n-Al has a significant portion of dead mass due to its relatively thick native oxide layer (2–6 nm) [28]. n-Al is of safety concern due to its sensitivity to electrostatic discharge, mechanical, and friction impact [29]. Moreover, n-Al particles are subject to agglomeration, resulting in reduced specific surface area [30–32]. Given these concerns of n-Al, thermites composed of micron-Al (m-Al) remain highly relevant to practical applications. There is a still great need to improve the ignition and combustion properties of m-Al based thermites, for which the typical approach is to coat m-Al with fluoride or to use energetic additives. For example, Sippel et al. mixed m-Al with fluorine-based additives to reduce Al agglomeration during combustion and promote gas generation and burning rate [33]. Ohkura et al. reduced the minimum flash ignition energy of m-Al by the addition of WO_3 nanoparticles, which have better light absorption [34]. Ilunga et al. [35] and Parimi et al. [36] sensitized m-Al/CuO thermite with more reactive energetic additives (Si/Bi_2O_3 thermites [35] and porous-$Si/NaClO_4$ [36], respectively).

Those pioneering work indeed demonstrated the potential to improve the ignition and combustion of m-Al, but there is a lack of systematic study to investigate how the synthesis method affects the morphology of m-Al thermites and how the morphology further influences their ignition and combustion properties. The importance of such a study was already demonstrated for n-Al thermites by Monk et al. [32], and this study demonstrated that the synthesis method of n-Al/CuO thermites (in the form of nanocomposites) significantly impact their combustion behaviors in different gas environments.

Herein, we investigate the effect of synthesis method on the morphology and ignition and combustion properties of m-Al based thermites. We choose Al/CuO as our model thermite system, as it is among the most investigated thermites due to their high energy density and reactivity [37–39]. For the synthesis, we focus on three synthesis methods that do not require any special equipment, *i.e.*, mechanical mixing (MM), the precipitation (PC) method and displacement (DP) method. We characterized the ignition and combustion performance of m-Al/CuO thermites prepared by these three methods by analyzing the trends observed in constant-volume vessel, bomb calorimetry, and differential scanning calorimetry tests. In general, PC- and DP-thermites have better dispersion and reduced diffusion distance of m-Al and CuO than MM-thermites, leading to shorter ignition delay and more efficient combustion. In particular, PC-thermites, with uniform dispersion and flocculent structures, exhibit the shortest ignition delay time, lowest reaction onset temperature, and highest amount of heat release.

2. Experimental methodology

Our objective is to study the effect of composition and morphology of m-Al/CuO thermites on their ignition and combustion properties. We will tune the morphology of m-Al/CuO thermites by using different synthesis methods. With the potential scalability in mind, we chose three simple synthesis methods to prepare m-Al/CuO thermites, *i.e.*, mechanical mixing, precipitation, and displacement methods, which are schematically illustrated in Fig. 1. These three methods do not require any special equipment but only beakers. The morphology and composition of the prepared thermite samples were characterized with scanning electron microscopy, energy-dispersive X-ray spectroscopy, X-ray diffraction, and inductively coupled plasma mass spectrometry. Their ignition and combustion properties were quantified with constant-volume vessel, bomb calorimetry, and differential scanning calorimetry.

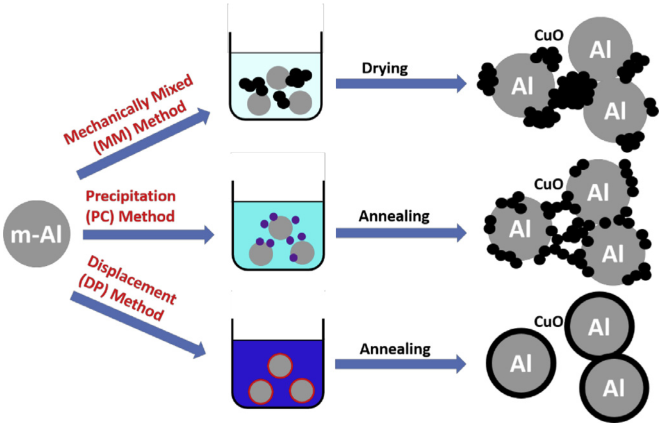

Fig. 1. The schematics of three different synthesis methods to prepare m-Al/CuO thermites and their expected morphologies.

2.1. Sample preparation methods for m-Al/CuO thermites

2.1.1. Mechanical mixing (MM) method

Mechanically mixed m-Al/CuO thermites were prepared as a control sample for comparison. For stoichiometric thermite mixtures ($2Al + 3CuO \rightarrow Al_2O_3 + 3Cu$), 100 mg of m-Al particles (99.8%, 3.0–4.5 µm in diameter, Alfa Aesar, also used in other preparation methods) and 442 mg of CuO particles ($<$ 50 nm in diameter, Sigma-Aldrich) were mixed in 15 ml of hexane and sonicated for 30 min. Then, the solvent hexane was vaporized at 80 °C for 1 h, and the particles were fully dried in a vacuum desiccator for 12 h.

2.1.2. Precipitation (PC) method

The PC method forms copper complex on top of m-Al particles. The copper complex is further converted to CuO by annealing. Since the copper complex might also precipitate in the solution, the final m-Al/CuO thermite will be a mixture of CuO and m-Al/CuO core/shell particles.

Specifically, to prepare stoichiometric Al/CuO thermite, first, 100 mg of m-Al particles were dispersed in 20 ml of anhydrous ethanol and sonicated for 10 min. Then, 4.5 ml of ammonium hydroxide solution (NH_4OH, 15%) was added into the suspension. After that, 12.9 ml of 100 g/l copper nitrate hemi(pentahydrate) ($Cu(NO_3)_2$-$2.5H_2O$, Sigma-Aldrich) ethanol solution was added into the suspension dropwise. After stirring for 3 h, the color of the suspension changed from gray to purple, indicating the formation of copper complex $Cu(NH_3)_4(OH)_2$ [40] in the solution and on the surface of m-Al. All the solid particles were collected by filtration and fully dried in a vacuum desiccator for 12 h. Finally, the dried particles were annealed on a hotplate at 250 °C for 20 min, and the color of the particles changed from purple to black, indicating the decomposition of $Cu(NH_3)_4(OH)_2$ to CuO [41].

2.1.3. Displacement (DP) method

The displacement method galvanically displaces Cu^{2+} by Al, forming Al/Cu core/shell particles. Then, Cu is further annealed to be CuO, forming m-Al/CuO core/shell particles.

Specifically, to prepare stoichiometric Al/CuO thermite, the $CuSO_4$-based stock solution was first prepared by dissolving 6 g of $CuSO_4$ (Sigma-Aldrich), 14 g of Ethylenediaminetetraacetic acid (EDTA, Sigma-Aldrich) and 28 g Triethanolamine (TEA, Sigma-Aldrich) in 1 l of de-ionized water. Then, NH_4OH aqueous solution

Please cite this article as: S. Deng et al., Tuning the morphological, ignition and combustion properties of micron-Al/CuO thermites through different synthesis approaches, Combustion and Flame (2018), https://doi.org/10.1016/j.combustflame.2018.04.028

was added into the $CuSO_4$ solution dropwise until pH = 9.7. Next, 100 mg of m-Al particles were added into 148 ml of the stock solution and sonicated for 1 min to form a well-dispersed suspension, and subsequently, this suspension was stirred for 5 min. During the stirring process, the color of the solution changed from blue to clear and the grayish Al particles turned red, indicating that Cu^{2+} is reduced to Cu on the surface of Al ($2Al + 3Cu^{2+} \rightarrow 2Al^{3+} + 3Cu$). These red particles were collected by filtration and washed by isopropanol. After fully dried in a vacuum desiccator for 12 h, these particles were annealed in a box furnace at 350 °C for 1 h under air ventilation. The color of the particles changed from red to black, indicating the conversion from Cu to CuO.

When we used these three methods to synthesize m-Al/CuO thermites of other equivalence ratios, we followed similar protocols but changed the mass ratio of Al and Cu precursors accordingly.

2.1.4. Expected morphologies of the thermite samples prepared by these methods

As shown in Fig. 1, the m-Al/CuO thermite prepared by MM is expected to have local agglomeration of Al and/or CuO [11,30], because sonication cannot fully break all the particle clusters and achieve uniform mixing. Also, the contact between Al and CuO is mainly physical and not strong. Conversely, for PC and DP, Cu-containing species is chemically deposited on the surface of Al particles, so the diffusion distance between Al and CuO is reduced. For PC, CuO is expected to be in the form of fine particles as they are precipitated out of the solution (Fig. 1). Some Cu complex are precipitated in the solution, and they will not be coated on m-Al but will still be collected into the final sample. For DP, the CuO is expected to be a dense shell since Al is displaced by Cu on the surface of m-Al particles and the Al/Cu undergoes a high temperature annealing process to form Al/CuO (Fig. 1). Since the final color of $CuSO_4$ stock solution is transparent, we expect that nearly all the Cu^{2+} cations in the solution have been reduced to Cu and coated on the surface of m-Al.

2.2. Characterization of the morphology and composition of m-Al/CuO

The morphology and element distribution of the m-Al/CuO thermites were characterized by scanning electron microscopy (SEM, FEI XL30 Sirion) with energy-dispersive X-ray spectroscopy (EDXS). The crystal phase and chemical compositions of all the samples were analyzed by X-ray diffraction (XRD, PANalytical X'Pert PRO). The equivalence ratio was determined by measuring the mass ratios of Al and Cu in each sample by inductively coupled plasma mass spectrometry (ICP-MS, Thermo Scientific XSERIES 2), assuming that Cu is present only in the form of CuO. The ICP-MS system was first calibrated with standard solutions (ICP multi-element standard solution VIII, Sigma-Aldrich). Then, 1 mg of each m-Al/CuO thermite was dissolved into 50 ml of 2% nitric acid at room temperature, and 15 ml of this sample solution was loaded into the test system following the standard operation procedures. After testing every ten sample solutions, a quality control solution was tested to validate the calibration.

2.3. Characterization of the ignition and combustion properties of m-Al/CuO

For all the ignition and combustion tests, the as-prepared thermite samples were first sieved through a mesh (US Standard Sieve Series No. 325) to break up large clusters and to obtain particles smaller than 45 µm.

2.3.1. Ignition delay and pressure rise measurement in a constant-volume vessel

We used a constant-volume vessel (volume: 13.5 cm^3) to determine the ignition delay time and pressure rise of various m-Al/CuO thermite samples. The constant-volume vessel is commonly used to investigate the combustion progress of thermites, and its schematics can be found in our previous work [36]. For a typical test, 30 mg of m-Al/CuO particles were loaded in a 100 µl alumina crucible with a hotwire (NiCr heating filament) embedded at the bottom. The sample was mechanically agitated in the alumina crucible to achieve a uniform porosity (86.6% for $\Phi = 2$ samples) before the test. The vessel initially contains ambient air. A constant current of 3.15 A was applied to the hotwire for ignition. The dynamic pressure from combustion was recorded by a pressure transducer (603B1, Kistler Inc.).

2.3.2. Heat of combustion measurement in a bomb calorimeter

The amount of heat release from various m-Al/CuO thermites, which is an indicator of combustion efficiency, was characterized by a bomb calorimeter (6725 Semi-micro Calorimeter, Parr Instrument Company). For a typically measurement, 100 mg of m-Al/CuO sample was placed on a pan with a NiCr filament embedded, achieving a similar porosity for samples with similar equivalence ratio by different methods (~85.8% for $\Phi = 2$ samples). The sample was encapsulated in a stainless-steel test cell. The test cell was flushed with helium to remove oxygen and to maintain atmospheric pressure during the test. The bomb calorimeter measurement provides the specific heat release of the thermite sample with the unit of kJ/g of thermite.

2.3.3. Reaction onset temperature measurement in a differential scanning calorimeter

The isothermal ignition behavior of various m-Al/CuO thermites was investigated by differential scanning calorimetry (DSC, Setaram Labsys Evo). For each test, 5 mg of sample particles were placed in a 100 µl alumina crucible. The porosity is similar for samples with similar equivalence ratio (~88.2% for samples with $\Phi = 2$ by different methods). The DSC chamber was first flushed with argon (100 sccm) for 30 min to remove the residual oxygen, and then the sample was heated in an inert argon environment (40 sccm) from room temperature to 1100 °C at a heating rate of 10 °C/min. After cooling down to room temperature, the sample was reheated with the same process, and the reheating curve was used to correct the baseline of the first heating process [36,42]. The baseline correction is necessary because the specific heat capacity of the sample changes as the reactants are converted to products.

3. Results and discussion

3.1. Material morphology and composition characterization

Figure 2 plots the actual equivalence ratio determined by ICP-MS versus the theoretical equivalence ratio calculated from the precursor mass compositions. For MM-thermites, the two equivalence ratios are the same as expected. For PC-thermites, the actual equivalence ratio is higher since not all the Cu precursor is precipitated and utilized. For DP-thermites, the actual equivalence ratio is lower since Al is consumed and dissolved in the alkaline solution during the displacement process. Overall, the deviation between actual and theoretical equivalence ratio is less than 20% for PC and DP methods. These correlations (Fig. 2) are then used to choose precursor mass compositions to prepare thermites with the desired equivalence ratio. It should be noted that we use the actual measured equivalence ratio (Φ) by ICP-MS hereafter for all the discussion to illustrate its effect on the morphology and performance of m-Al/CuO thermites.

Please cite this article as: S. Deng et al., Tuning the morphological, ignition and combustion properties of micron-Al/CuO thermites through different synthesis approaches, Combustion and Flame (2018), https://doi.org/10.1016/j.combustflame.2018.04.028

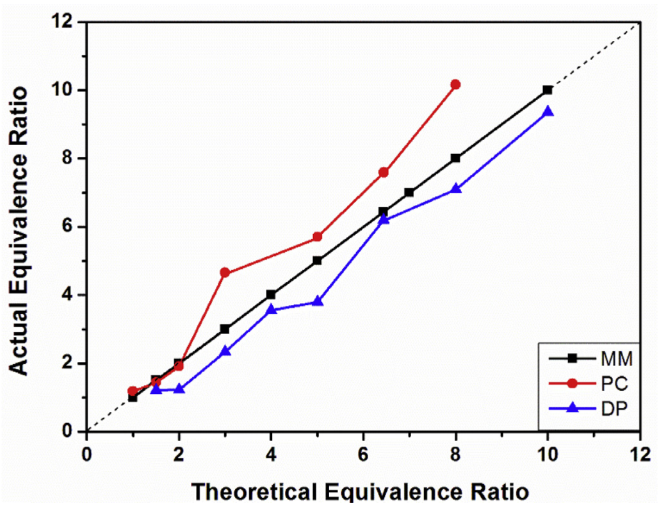

Fig. 2. The actual equivalence ratio measured by ICP-MS versus the theoretical equivalence ratio calculated from precursor compositions for three synthesis methods.

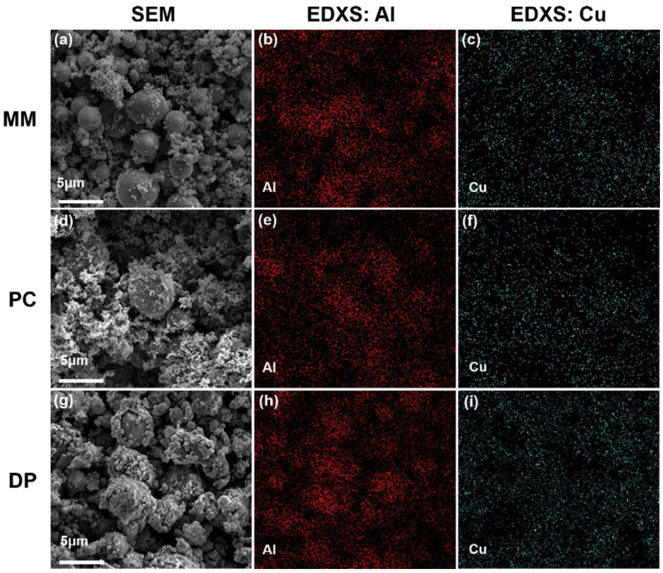

Fig. 3. SEM and EDXS images of m-Al/CuO thermites ($\Phi = 7$) prepared by the MM, PC, and DP methods.

Figure 3 compares the morphology and element distribution of Al and Cu of m-Al/CuO thermites ($\Phi = 7$) prepared by the MM, PC, and DP methods. The EDXS signals of both Al and Cu elements are uniform in the view globally for all three samples (Fig. 3). Nevertheless, the SEM images reveal their structural differences. For MM-thermites (Fig. 3a), m-Al can be clearly identified as large particles with rather smooth surface. Small amount of CuO nanoparticles are attached to the surface of m-Al, but most are agglomerates and lie in between m-Al particles. For PC-thermites (Fig. 3d), the precipitated CuO particles are nanoporous and less agglomerated and they mostly cover the surface of m-Al particles. For DP-thermites (Fig. 3g), CuO presents in the form of a dense shell coated around m-Al. The estimated averaged CuO shell thickness based on the SEM images varies from 1 μm to 100 nm for Φ from 1 to 9. These SEM images show that PC- and DP-thermites have better dispersion of m-Al and CuO than MM-thermites. PC-thermites have more nanostructured CuO than DP-thermites. These morphology differences among the m-Al/CuO thermites are expected to lead to different ignition and combustion behaviors. We further measured the specific surface area (SSA) of these samples with BET, and the results show that the PC sample has the largest SSA (6.3 m^2/g), which could be attributed to the reduced agglomeration and/or finer CuO particles. MM sample exhibits the smallest SSA (3.7 m^2/g), revealing the severe agglomeration of CuO particles in the thermites. While CuO in the DP sample exists in the form of a condensed shell, DP sample shows an SSA (4.6 m^2/g) higher than MM, which may be due to the reduced agglomeration and the rough surface of the CuO shell. The BET results are consistent to the images of SEM.

Figure 4 shows the XRD spectra of m-Al/CuO thermites prepared by the three synthesis methods for $\Phi = 2$ and 7. For these six samples, all the XRD peaks are assigned to either Al or CuO, confirming that all three synthesis methods have achieved the desired chemical compositions. The XRD intensity ratio between Al and CuO for $\Phi = 2$ (Fig. 4a) is smaller than that of $\Phi = 7$ (Fig. 4b), which is consistent with the smaller Al to CuO mass ratio for $\Phi = 2$.

3.2. Ignition and combustion characterization

3.2.1. Ignition delay time and peak pressure measured in the constant-volume vessel

We use a constant-volume vessel with a hotwire igniter to determine both the ignition delay time and pressure release of thermites. Representative pressure time history plots are shown in Fig. 5. The ignition delay time is defined as the time difference between the initiation of the constant current applied to the hotwire and the rise of pressure (typically 3 kPa, but the choice of this threshold value does not affect the qualitative trend) detected by the pressure transducer. The peak pressure is defined as the maximum pressure recorded during combustion. Figure 5 shows that the ignition delay time increases in the sequence of PC < DP < MM for the slightly fuel-rich condition ($\Phi = 2$) and in the sequence of DP < PC < MM for the very fuel-rich condition ($\Phi = 7$). Clearly, the synthesis method affects the ignition delay time differently for different equivalence ratios, and the same applies to the peak pressure. Details about the effects on ignition delay time and peak pressure are discussed in the following paragraphs.

To facilitate the comparison, Fig. 6 plots the measured ignition delay time as a function of Φ for thermites prepared by the three different synthesis methods. First, for the entire equivalence ratio Φ range from 1 to 10 investigated, the ignition delay time of PC- (red circles) and DP-thermites (blue triangles) is smaller than that of MM-thermites (black squares), confirming that better mixing between Al and CuO facilitates ignition. Second, the equivalence ratio Φ in Fig. 6 can be further divided into two regions. In Region I ($\Phi < 4.5$), PC-thermite has smaller ignition delay than that of DP-thermite. The reason is that, in both cases, CuO is relatively abundant and in close contact with m-Al particles. However, the CuO for PC-thermite is more porous than that for DP-thermite, so the former can provide oxygen more readily and allow combustion product to diffuse out more efficiently. In contrast, for Region II ($\Phi > 4.5$), CuO is rather scarce so the proximity and contact area between Al and CuO are more crucial to ignition. Therefore, DP-thermites have the shortest ignition delay time. Third, both MM- and PC-thermites achieve the shortest ignition delay time under slightly fuel-rich condition ($\sim \Phi = 2$). This rich-shift for m-Al/CuO thermites is consistent with previous results [14,43,44]. Previous equilibrium calculation showed that the adiabatic flame temperature of Al and CuO peaks at $\Phi = 1.05$ [14]. The best performance of nano-Al/CuO (in terms of burning rates, propagation speeds, and pressure generation measured in various apparatus) peaks around $\Phi = 1.2$ to 1.9 [14,43,44]. The amount of rich-shift for m-Al/CuO thermites here should be more than previously studied nano-Al/CuO, since m-Al particles generally react less completely

Please cite this article as: S. Deng et al., Tuning the morphological, ignition and combustion properties of micron-Al/CuO thermites through different synthesis approaches, Combustion and Flame (2018), https://doi.org/10.1016/j.combustflame.2018.04.028

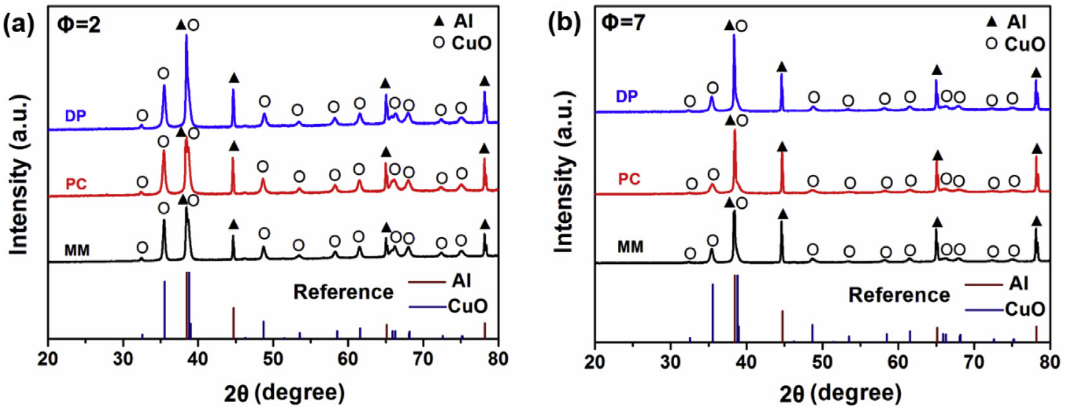

Fig. 4. XRD spectra of m-Al/CuO thermites with equivalence ratio $\Phi = 2$ and 7 prepared by three synthesis methods. Reference: Al (ICDD 00-004-0787) and CuO (ICDD 01-070-6829).

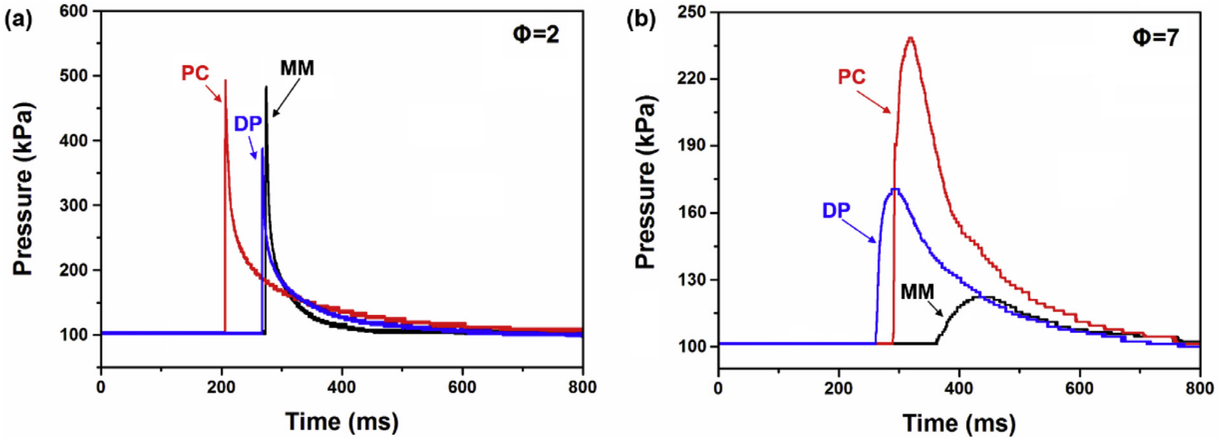

Fig. 5. The time history of the pressure in the constant-volume vessel for m-Al/CuO thermites with equivalence ratio (a) $\Phi = 2$ and (b) $\Phi = 7$ prepared by three synthesis methods.

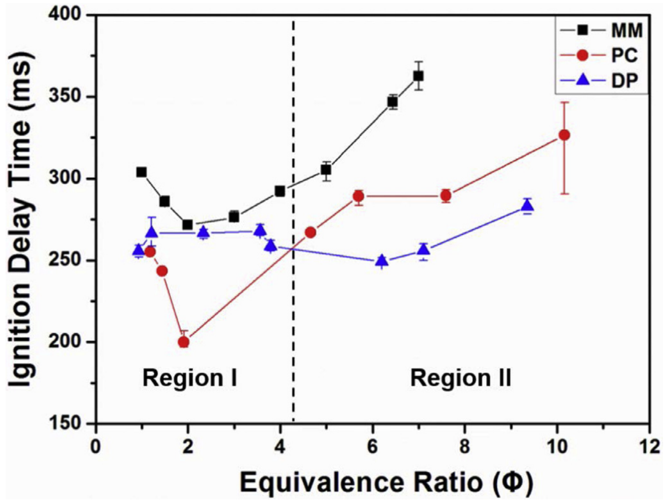

Fig. 6. The ignition delay time of m-Al/CuO thermites as a function of equivalence ratio for three synthesis methods. (For interpretation of the references to color in this figure, the reader is referred to the web version of this article.)

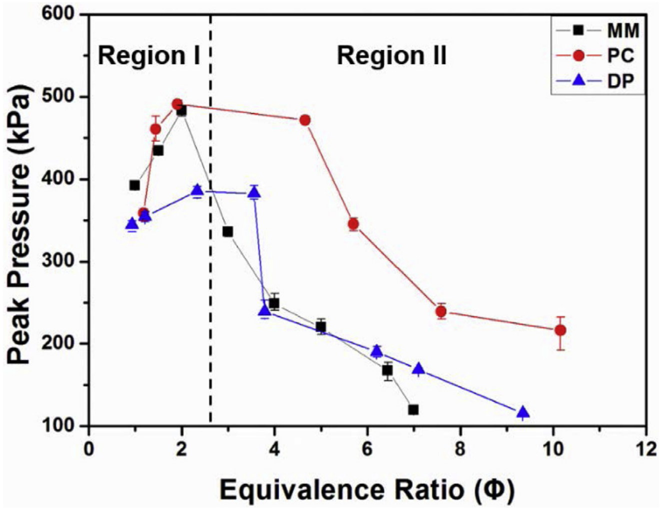

Fig. 7. The peak pressure of m-Al/CuO thermites as a function of equivalence ratio for three synthesis methods.

than nano-Al. Finally, the ignition delay of DP-thermite is insensitive to Φ, since ignition is controlled by the interface between Al and CuO, which is nearly invariant with Φ for the core/shell DP-thermites (Fig. 3g).

Figure 7 plots the measured peak pressure as a function of Φ for samples prepared by three different synthesis methods. The pressure rise is caused by both the gas production and thermal expansion from the thermite reaction, which is an indicator for the combustion intensity and efficiency. First, for samples prepared by

Please cite this article as: S. Deng et al., Tuning the morphological, ignition and combustion properties of micron-Al/CuO thermites through different synthesis approaches, Combustion and Flame (2018), https://doi.org/10.1016/j.combustflame.2018.04.028

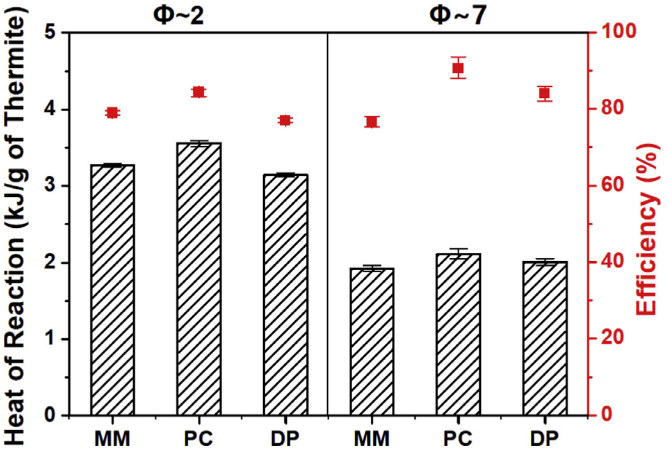

Fig. 8. Comparison of the specific heat of reaction and combustion efficiency of m-Al/CuO thermites prepared by three synthesis methods with the equivalence ratios of 2 and 7.

all three synthesis methods, the peak pressure during combustion peaks around $\Phi = 2$. This indicates that the optimal combustion efficiency is mainly determined by Φ when the morphology is similar. The optimal combustion condition of $\Phi = 2$ also matches with the optimal ignition condition of $\Phi = 2$ in Fig. 6. Second, the equivalence ratio Φ in Fig. 7 can also be divided into two regions. In Region I ($\Phi < 2.5$), the trend of the peak pressure is $PC \approx MM > DP$ for the same Φ. In Region II ($\Phi > 2.5$), the peak pressure trend is $PC > DP \geq MM$. PC-thermite has the highest peak pressure in both regions. The reason is that combustion is more sensitive to the morphology of CuO, rather than the interface distance between Al and CuO. After ignition, CuO decomposes and releases O_2, which is a key factor contributing to the pressure rise. Hence, CuO with large specific surface area, such as in PC-thermite, will have a higher pressure rise. Finally, DP-thermite has the best core/shell structure but the lowest peak pressure for relative lower Φ. One possible explanation is that the CuO shell is rather dense and thick at these equivalence ratios, so the generated gaseous products at the Al/CuO interface cannot easily escape from the shell, inhibiting further reactions. The inhibiting effect gets less pronounced as the CuO shell gets thinner for higher Φ.

3.2.2. Ignition and combustion performance of the best thermites of $\Phi = 2$ and the most fuel rich cases of $\Phi = 7$

The above results show that m-Al/CuO of $\Phi = 2$ has the lowest ignition delay (Fig. 6) and the highest peak pressure (Fig. 7).

When applications desire high amount of loading of m-Al, rich thermite, such as m-Al/CuO of $\Phi = 7$, is of interests since it has smaller amount of CuO. For $\Phi = 7$, CuO can be regarded as a sensitizer to initiate and promote m-Al combustion with other oxidizers such as air. Due to the importance of both $\Phi = 2$ and 7 cases, we conducted additional experiments to further characterize their ignition and combustion properties. We conducted these experiments under inert environment to assess the sole exothermicity and onset temperature of m-Al/CuO thermite reactions by eliminating the reactions between m-Al and air.

The experimental heat of reaction of six thermite samples ($\Phi = 2$ and 7, each case includes MM, PC and DP sample) in an inert environment (helium) was determined with bomb calorimetry and plotted in Fig. 8, where the error bars indicate the sample variation. The efficiency of combustion, which is defined as the ratio of experimental heat of reaction to the theoretical heat of reaction, was also presented. The overall trend of heat of reaction and combustion efficiency are similar to those of peak pressure in Fig. 7. PC-thermites have higher efficiency of combustion since their CuO has a flocculent structure with better dispersion and finer clusters. Under the slightly fuel-rich condition ($\Phi = 2$), DP-thermite exhibits the lowest combustion efficiency due to the dense Al_2O_3 layer formed during the reaction that prevents further combustion. However, under the fuel-richer condition ($\Phi = 7$), as the thickness of CuO decreases, such a prohibiting effect becomes less pronounced. The core/shell structure of DP-thermite is beneficial to reducing diffusion distance and hence promoting reaction between m-Al and CuO. Consequently, the DP-thermite sample has a higher heat of reaction as well as combustion efficiency than the MM-thermite. The increasing combustion efficiency of PC and DP samples from $\Phi = 2$ to $\Phi = 7$ also demonstrates the advantages of PC and DP methods for Al/CuO under fuel-richer condition, which is due to the reduced agglomeration of CuO (PC) and thinner CuO shell (DP).

We also quantified the reaction onset temperatures of the six samples in DSC under slow heating conditions to compare to the trend of faster heating of the hotwire in the constant-volume vessel. The DSC heat flow curves are plotted in Fig. 9, in which the endothermic peak at 660 °C corresponds to the melting Al. For all cases, there are a small exothermic peak before the Al melting peak and a larger one after, which come from different stages of Al oxidization.

For the first exothermic peak, the slight right-shift (~20–30 °C) of the first small peak in PC and DP may be due to two possible reasons. First, this peak is likely to be associated with n-Al oxidation, for n-Al would have shorter diffusion length than m-Al

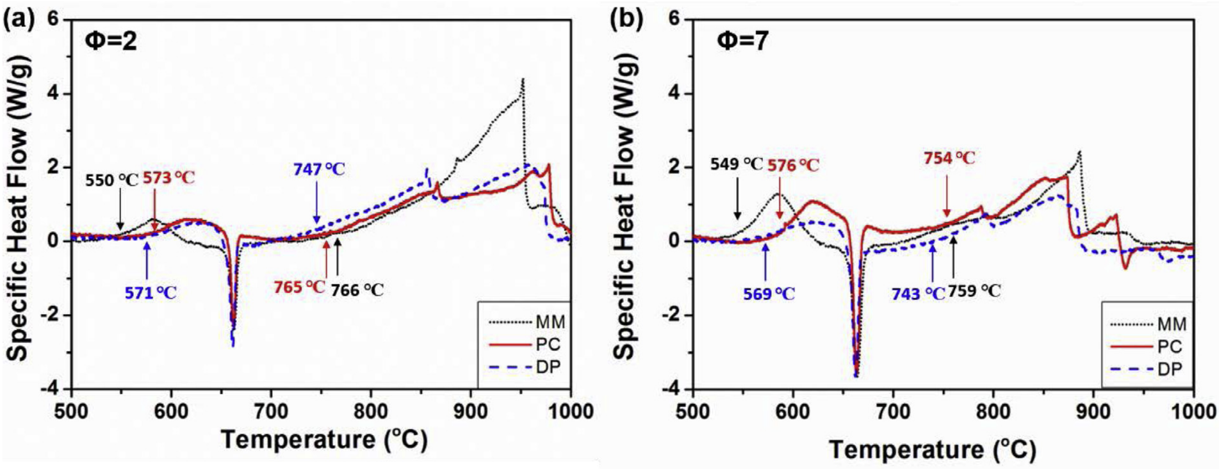

Fig. 9. The specific heat flow of m-Al/CuO thermites prepared by different synthesis methods with the equivalence ratios of 2 and 7.

Please cite this article as: S. Deng et al., Tuning the morphological, ignition and combustion properties of micron-Al/CuO thermites through different synthesis approaches, Combustion and Flame (2018), https://doi.org/10.1016/j.combustflame.2018.04.028

Table 1
The average particle size and size distribution of the as-received m-Al particles.

Average particle size	D_{10}	D_{50}	D_{90}
3.90 µm	2.21 µm	4.57 µm	10.38 µm

and hence lower onset temperature. The as-received m-Al particles have a size distribution shown in Table 1. Therefore, the loss of nano-particles of Al during the synthesis of PC and DP may lead to such right-shift of first peak in DSC. Second, the onset temperature of first peak has been reported to be associated with phase transformation from amorphous alumina to γ-Al_2O_3 [5,6,45]. During the synthesis of PC, a thin layer of alumina of another phase may have formed due to chemical reaction or annealing, and therefore, the first exothermic peak may be slightly postponed. Similar reason may also apply to the DP sample, as a thin layer of crystalline aluminum oxide or aluminum copper alloy may be formed during synthesis or annealing and thus postpone the first exothermic peak in DSC. However, the scope of our current study is focused on investigating how the synthesis method affect the morphological and thermal properties of m-Al particles. Besides, under fast heating conditions, the thermites are heated above the melting point of Al very rapidly, so this slight right-shift should be negligible.

The onset temperature of the second exothermic peak is in the narrow range of 743 to 765 °C. The similar onset temperature is likely due to the fact that Al has melted above 660 °C, so the initial morphology is less important. Compared to the large ignition delay difference observed in Fig. 5, the results indicate that morphology plays a more important role for the fast heating case.

4. Conclusions

We developed two simple synthesis methods (*i.e.*, precipitation and displacement methods) to prepare micron-sized Al/CuO thermites. Both methods produce thermites with reduced agglomeration and shorter diffusion distance than the common mechanically mixed thermites. Their ignition and combustion properties were characterized by the constant-volume vessel, bomb calorimetry, and differential scanning calorimetry tests. In general, PC- and DP-thermites have shorter ignition delay and higher combustion efficiency than MM-thermites. PC thermites, specifically, exhibit the shortest ignition delay time, lowest reaction onset temperature, and highest amount of heat release due to their flocculent structures. DP-thermites exhibit distinct ignition properties in that their ignition delay is rather insensitive to the equivalence ratio. Regardless of the synthesis method, m-Al/CuO thermites with $\Phi = 2$ show the best ignition and combustion behavior. Finally, both PC and DP methods only use beakers for synthesis and are potentially scalable. Both methods demonstrate good control over the desired chemical composition and morphology of the obtained thermites. Hence, we believe that similar precipitation and displacement methods are applicable to modify the morphology of various other thermites (varying compositions and sizes) with enhanced uniformity and interface between metal fuels and oxidizers.

Acknowledgments

This work was supported by Army Research Office under the Agreement number W911NF-14-1-0271 and the Office of Naval Research under the Agreement number N00014-15-1-2028.

References

[1] K.P. Brooks, M.W. Beckstead, Dynamics of aluminum combustion, J. Propuls. Power 11 (1995) 769–780.
[2] L.L. Wang, Z.A. Munir, Y.M. Maximov, Thermite reactions: their utilization in the synthesis and processing of materials, J. Mater. Sci. 28 (1993) 3693–3708.
[3] P. Bucher, R.A. Yetter, F.L. Dryer, E.P. Vicenzi, T.P. Parr, D.M. Hanson-Parr, Condensed-phase species distributions about Al particles reacting in various oxidizers, Combust. Flame 117 (1999) 351–361.
[4] Y. Gan, L. Qiao, Combustion characteristics of fuel droplets with addition of nano and micron-sized aluminum particles, Combust. Flame 158 (2011) 354–368.
[5] M.A. Trunov, M. Schoenitz, X. Zhu, E.L. Dreizin, Effect of polymorphic phase transformations in Al_2O_3 film on oxidation kinetics of aluminum powders, Combust. Flame 140 (2005) 310–318.
[6] M.A. Trunov, M. Schoenitz, E.L. Dreizin, Effect of polymorphic phase transformations in alumina layer on ignition of aluminum particles, Combust. Theory Model 10 (2006) 603–623.
[7] V.I. Rozenband, N.I. Vaganova, A strength model of heterogeneous ignition of metal particles, Combust. Flame 88 (1992) 113–118.
[8] E.W. Price, Effect of multidimensional flamelets in composite propellant combustion, J. Propuls. Power 11 (1995) 717–729.
[9] V.A. Babuk, V.A. Vasilyev, Model of aluminum agglomerate evolution in combustion products of solid rocket propellant, J. Propuls. Power 18 (2002) 814–823.
[10] D. Sundaram, V. Yang, R.A. Yetter, Metal-based nanoenergetic materials: synthesis, properties, and applications, Prog. Energy Combust. Sci. 61 (2017) 293–365.
[11] E.L. Dreizin, Metal-based reactive nanomaterials, Prog. Energy Combust. Sci. 35 (2009) 141–167.
[12] A. Prakash, A.V. McCormick, M.R. Zachariah, Synthesis and reactivity of a super-reactive metastable intermolecular composite formulation of Al/$KMnO_4$, Adv. Mater. 17 (2005) 900–903.
[13] M.L. Pantoya, J.J. Granier, Combustion behavior of highly energetic thermites: nano versus micron composites, Propellants Explos. Pyrotech. 30 (2005) 53–62.
[14] V.E. Sanders, B.W. Asay, T.J. Foley, B.C. Tappan, A.N. Pacheco, S.F. Son, Reaction propagation of four nanoscale energetic composites (Al/MoO_3, Al/WO_3, Al/CuO, and Bi_2O_3), J. Propuls. Power 23 (2007) 707–714.
[15] K.B. Plantier, M.L. Pantoya, A.E. Gash, Combustion wave speeds of nanocomposite Al/Fe_2O_3: the effects of Fe_2O_3 particle synthesis technique, Combust. Flame 140 (2005) 299–309.
[16] T.M. Tillotson, A.E. Gash, R.L. Simpson, L.W. Hrubesh, J.H. Satcher, J.F. Poco, Nanostructured energetic materials using sol–gel methodologies, J. Non-Cryst. Solids 285 (2001) 338–345.
[17] B. Mehendale, R. Shende, S. Subramanian, S. Gangopadhyay, P. Redner, D. Kapoor, S. Nicolich, Nanoenergetic composite of mesoporous iron oxide and aluminum nanoparticles, J. Energy Mater. 24 (2006) 341–360.
[18] S. Apperson, R.V. Shende, S. Subramanian, D. Tappmeyer, S. Gangopadhyay, Z. Chen, K. Gangopadhyay, P. Redner, S. Nicholich, D. Kapoor, Generation of fast propagating combustion and shock waves with copper oxide/aluminum nanothermite composites, Appl. Phys. Lett. 91 (2007) 243109.
[19] F. Séverac, P. Alphonse, A. Estève, A. Bancaud, C. Rossi, High-energy Al/CuO nanocomposites obtained by DNA-directed assembly, Adv. Funct. Mater. 22 (2012) 323–329.
[20] Y. Tao, J. Zhang, Y. Yang, H. Wu, L. Hu, X. Dong, J. Lu, S. Guo, Metastable intermolecular composites of Al and CuO nanoparticles assembled with graphene quantum dots, RSC Adv. 7 (2017) 1718–1723.
[21] A.J. Gavens, D. Van Heerden, A.B. Mann, M.E. Reiss, T.P. Weihs, Effect of intermixing on self-propagating exothermic reactions in Al/Ni nanolaminate foils, J. Appl. Phys. 87 (2000) 1255–1263.
[22] K.J. Blobaum, M.E. Reiss, J.M. Plitzko, T.P. Weihs, Deposition and characterization of a self-propagating CuOx/Al thermite reaction in a multilayer foil geometry, J. Appl. Phys. 94 (2003) 2915–2922.
[23] J. Wang, E. Besnoin, A. Duckham, S.J. Spey, M.E. Reiss, O.M. Knio, M. Powers, M. Whitener, T.P. Weihs, Room-temperature soldering with nanostructured foils, Appl. Phys. Lett. 83 (2003) 3987–3989.
[24] Y. Ohkura, S.-Y. Liu, P.M. Rao, X. Zheng, Synthesis and ignition of energetic CuO/Al core/shell nanowires, Proc. Combust. Inst. 33 (2011) 1909–1915.
[25] M. Schoenitz, T.S. Ward, E.L. Dreizin, Fully dense nano-composite energetic powders prepared by arrested reactive milling, Proc. Combust. Inst. 30 (2005) 2071–2078.
[26] S.M. Umbrajkar, S. Seshadri, M. Schoenitz, V.K. Hoffmann, E.L. Dreizin, Aluminum-rich Al-MoO_3 nanocomposite powders prepared by arrested reactive milling, J. Propuls. Power 24 (2008) 192–198.
[27] Y.F. Ivanov, M.N. Osmonoliev, V.S. Sedoi, V.A. Arkhipov, S.S. Bondarchuk, A.B. Vorozhtsov, A.G. Korotkikh, V.T. Kuznetsov, Productions of ultra-fine powders and their use in high energetic compositions, Propellants Explos. Pyrotech. 28 (2003) 319–333.
[28] R.A. Yetter, G.A. Risha, S.F. Son, Metal particle combustion and nanotechnology, Proc. Combust. Inst. 32 (2009) 1819–1838.
[29] R. Thiruvengadathan, G.M. Belarde, A. Bezmelnitsyn, M. Shub, W. Balas-Hummers, K. Gangopadhyay, S. Gangopadhyay, Combustion characteristics of silicon-based nanoenergetic formulations with reduced electrostatic discharge sensitivity, Propellants Explos. Pyrotech. 37 (2012) 359–372.
[30] D. Wei, R. Dave, R. Pfeffer, Mixing and characterization of nanosized powders: an assessment of different techniques, J. Nanopart. Res. 4 (2002) 21–41.
[31] H. Wang, G. Jian, G.C. Egan, M.R. Zachariah, Assembly and reactive properties of Al/CuO based nanothermite microparticles, Combust. Flame 161 (2014) 2203–2208.

Please cite this article as: S. Deng et al., Tuning the morphological, ignition and combustion properties of micron-Al/CuO thermites through different synthesis approaches, Combustion and Flame (2018), https://doi.org/10.1016/j.combustflame.2018.04.028

[32] I. Monk, M. Schoenitz, R.J. Jacob, E.L. Dreizin, M.R. Zachariah, Combustion characteristics of stoichiometric Al–CuO nanocomposite thermites prepared by different methods, Combust. Sci. Technol. 189 (2017) 555–574.

[33] T.R. Sippel, S.F. Son, L.J. Groven, Aluminum agglomeration reduction in a composite propellant using tailored Al/PTFE particles, Combust. Flame 161 (2014) 311–321.

[34] Y. Ohkura, P.M. Rao, I. Sun Cho, X. Zheng, Reducing minimum flash ignition energy of Al microparticles by addition of WO_3 nanoparticles, Appl. Phys. Lett. 102 (2013) 43108.

[35] K. Ilunga, O. del Fabbro, L. Yapi, W.W. Focke, The effect of Si–Bi_2O_3 on the ignition of the Al–CuO thermite, Powder Technol. 205 (2011) 97–102.

[36] V.S. Parimi, S. Huang, X. Zheng, Enhancing ignition and combustion of micron-sized aluminum by adding porous silicon, Proc. Combust. Inst. 36 (2017) 2317–2324.

[37] S. Hasani, M. Panjepour, M. Shamanian, The oxidation mechanism of pure aluminum powder particles, Oxid. Met. 78 (2012) 179–195.

[38] E. Lafontaine, M. Comet, Nanothermites, John Wiley & Sons, Inc., Hoboken, NJ, USA, 2016.

[39] O. Mulamba, M. Pantoya, Oxygen scavenging enhances exothermic behavior of aluminum-fueled energetic composites, J. Therm. Anal. Calorim. 116 (2014) 1133–1140.

[40] W. Li, H. Cheng, $Bi_2O_3/CuCr_2O_4$–CuO core/shell structured nanocomposites: facile synthesis and catalysis characterization, J. Alloys Compd. 448 (2008) 287–292.

[41] Y. Ohkura, Synthesis and optical ignition of aluminum and silicon-based energetic materials, Stanford University, 2013 Ph.D..

[42] S. Huang, S. Deng, Y. Jiang, J. Zhao, X. Zheng, Electroless deposition and ignition properties of Si/Fe_2O_3 core/shell nanothermites, ACS Omega 2 (2017) 3596–3600.

[43] N.H. Yen, L.Y. Wang, Reactive metals in explosives, Propellants Explos. Pyrotech. 37 (2012) 143–155.

[44] K.T. Sullivan, J.D. Kuntz, A.E. Gash, Electrophoretic deposition and mechanistic studies of nano-Al/CuO thermites, J. Appl. Phys. 112 (2012) 24316.

[45] M.L. Pantoya, J.J. Granier, The effect of slow heating rates on the reaction mechanisms of nano and micron composite thermite reactions, J. Therm. Anal. Calorim. 85 (2006) 37–43.

Please cite this article as: S. Deng et al., Tuning the morphological, ignition and combustion properties of micron-Al/CuO thermites through different synthesis approaches, Combustion and Flame (2018), https://doi.org/10.1016/j.combustflame.2018.04.028